HIGH-PERFORMANCE MATERIALS FOR MASK-PROJECTION STEREOLITHOGRAPHY VIA IN-SITU SEQUENTIAL INTERPENETRATING NETWORK

Anh N. Huynh, Nicolas J. Alvarez, Giuseppe R. Palmese
Drexel University
Philadelphia, PA/USA

ABSTRACT

Stereolithography, a common technique used in additive manufacturing, offers high dimensional accuracy. However, there are limited choices of materials for this process. Acrylates and epoxies are commonly used, but their thermal properties are not suitable for applications in which high temperature performance is needed. In contrast, high-performance thermosets such as bismaleimide and cyanate ester are cured using high temperature processing techniques, and their use for stereolithography is limited. In this work, a photocurable formulation of bismaleimide, a reactive diluent, and cyanate ester was developed to improve thermal and mechanical properties as well as cure shrinkage of stereolithography resins. *In-situ* sequential interpenetrating polymer network (IPN) were investigated wherein the copolymerization reaction between bismaleimide and diluent occurs during printing, resulting in a cyanate ester swollen network with sub room temperature glass transition temperature (T_g). The polymerization of cyanate ester takes place during post processing. The resulting material possesses a T_g well above 200ºC (loss modulus peak), significant decrease in cure shrinkage, and improved toughness.

Keywords: 3D printing, interpenetrating polymer network, high temperature, shrinkage
Corresponding author: Giuseppe R. Palmese, grp27@drexel.edu

1. INTRODUCTION

Additive manufacturing has gained great popularity in recent years due to its advantages such as design freedom, customization, waste reduction, and low cost.[1] Stereolithography processes (SLA) and derivatives, like mask-projection stereolithography, are popular techniques in additive manufacturing due to their ability to provide prints with high resolution. The materials used for this process are constrained by photo-curing chemistry and are typically acrylates, methacrylates, and epoxies.[2] Therefore, the use of materials with high thermal properties are limited. Recently, direct ink writing (DIW) of cyanate ester with fillers was reported by Lewicki et al.[3] Other attempts in designing materials with high temperature stability using aromatic polyimides have demonstrated printability but have high dimensional shrinkage and poor mechanical properties.[4] There are few reports in the literature regarding the T_g of SLA materials, and the reported T_g's range from 87-160°C (tan delta).[5, 6] Parts processed by SLA can exhibit significant residual stress [7] because polymerization of thermosetting monomers results in cure shrinkage due to the formation of a covalent bonds.[8] During printing, residual stress is caused by material shrinkage while being restrained between substrates. Residual stress can result in warpage or delamination, which can affect mechanical properties of printed parts.[9] The degree of shrinkage depends on

Copyright 2020. Used by the Society of the Advancement of Material and Process Engineering with permission.

chemical structure and varies generally from 5–10% for common acrylates and methacrylates.[2] Another limitation of SLA is low extent of reaction during room temperature printing, particularly for high T_g systems. The reactions of thermosets are limited by vitrification so that the T_g attained during isothermal cure is close to the reaction temperature.[10] Lange et al. demonstrated that the photocurable materials can generate high residual stress because of significant shrinkage close to vitrification when the modulus increases significantly.[11] Our work focuses on interpenetrating polymer network (IPN) which utilize high-performance materials to improve thermal and mechanical properties, conversion during print, and shrinkage.

The use of IPNs for SLA has been reported. A common combination of chemistries used for the formation of sequential IPNs entails the free radical photopolymerization of acrylates followed by cationic polymerization of epoxies.[12,13] Another type of IPN used in SLA is the two-stage curing of acrylates and epoxies, where acrylates are photopolymerized, and the epoxies are thermally cured with a curing agent.[6] Our study utilizes two-stage curing but allows the processing of high-performance material that are traditionally thermally cured. Bismaleimide (BMI) and cyanate ester (CE) are not favorable for SLA as they require high curing temperature.[14-16] In addition, bismaleimide is a brittle material and generally requires toughening for more practical use. It is reported in literature that the formation of IPN between bismaleimide and cyanate ester provides a toughening effect.[17-19] A reactive diluent that can copolymerize with bismaleimide is needed in order to formulate a BMI-CE for SLA applications. Previous works showed that bismaleimide copolymerizes with acryloylmorpholine through electron donor acceptor mechanism under electron beam irradiation or UV irradiation in the presence of appropriate photoinitiators.[18,20] In this work, we investigate sequential IPNs wherein a first network of bismaleimide and acryloylmorpholine is formed during printing, and the second network of cyanate ester is obtained subsequently by thermal cure. The concept is demonstrated in Figure 1. This scheme is expected to result in delayed vitrification due to the presence of unreacted second network allowing a greater conversion of double bonds in the rubbery state and overall lower cure shrinkage because cyanate ester is known to have a low degree of shrinkage.[16]

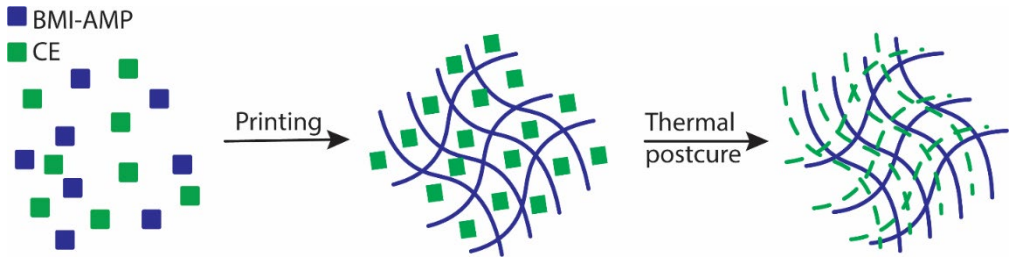


Figure 1: The reaction sequence in IPN.

2. EXPERIMENTATION

2.1 Resin preparation

Poly(phenylmethane) maleimide (kindly supplied by Miki Sangyo), 4-acryloylmorpholine (TCI Chemicals), bisphenol E cyanate ester AroCy L-10 (Huntsman), Copper (II) napthenate (Strem Chemicals), and phenyl bis(2,4,6trimethylbenzoyl) phosphine oxide (Sigma Aldrich) were used as received. Poly(phenylmethane) maleimide (BMI) was dissolved in 4-acrcyloylmorpholine (AMP) at 70 ºC at a concentration of 30 wt% BMI in AMP. Bisphenol-E cyanate ester (CE) was well

mixed with copper (II) napthenate at concentration of 200 ppm Cu^{2+}. The photoinitiator, phenyl bis(2,4,6 trimethylbenzoyl) phosphine oxide (PPO), was dissolved in the resins at a concentration of 0.5 wt.% with respect to the total mass of the resin. Two resin systems were investigated: (1) 30 wt% BMI in AMP and (2) the IPN resin composed of 50 wt% of system (1) and 50 wt% of cyanate ester. Throughout the paper, system (1) is denoted as BMI-AMP and system (2) is denoted as IPN 50:50 (BMI-AMP):CE.

2.2 Printing and post-curing procedures

The resins were printed using Anycubic Photon printer with the LED light of 405 nm. The power density of the light measured at LCD surface was 0.51 mW/cm^2 (measured by ILT 2400 with sensor range of 275–450 nm). Both resins were printed using 100-micron layer thickness with 80 s exposure per layer. The printed samples were first post-cured in a UV oven (FormLabs) at 75 ºC for 1 hr. The BMI -AMP system was then thermally post-cured at 120 ºC for 3 hrs, 180 ºC for 3 hrs, 220 ºC for 4hrs, and 280 ºC 1 hr. The IPN system was post-cured at 150 ºC for 2 hrs, 180 ºC overnight, 220 ºC for 3 hrs, and 280 ºC for 1 hr. The thermal postcuring procedures were divided into multiple temperature stages in order to prevent the evaporation of AMP and the highly exothermic reaction of cyanate ester.

2.3 Polymer characterizations

The T_g was measured by Dynamic Mechanical Analysis using a TA Instruments DMA 2980. typical size was 35 x 12 x 3.2 mm. The tests were carried out using single cantilever mode with amplitude of 10 μm, frequency 1 Hz, and a temperature ramp rate of 2 ºC/min. Sample dimensions were 35 x 12 x 3.2 mm.

The density of printed and postcured parts were measured using a density gradient column following ASTM 1505-03. Samples were rinsed with water before being placed in the column, and the position of the sample was recorded after 2 hours of submersion. The volumetric shrinkage was calculated using the following equation:

$$volumetric\ shrinkage = 100 * \frac{(density\ at\ cure\ stage - resin\ density)}{resin\ density} \quad (1)$$

Mechanical tests were performed at room temperature using an Instron Model 8872. The compact tension samples, followed ASTM 5045-99, had the dimension of 15.5 x 14.88 x 5.5 mm and the notch length of 8.7 mm. A crack was initiated at the bottom of the notch by a sharp razor blade. For each formulation, five to ten compact tension samples were tested at crosshead speed of 0.5 mm/min. The flexural tests were conducted following ASTM D790 in 3-point bending configuration to characterize the flexural strength and modulus using five samples per formulation with a span to depth ratio of 16:1. The flexural specimens had the dimension of 120 x 12.7 x 3.2 mm.

Fourier transform infrared (FTIR) spectroscopy in the mid infrared region (mid-IR) was used to evaluate the extent of cure of printed and post-cured parts. The C=C of AMP and BMI were characterized by peaks at 790 cm^{-1} and 690 cm^{-1}, respectively. The fractional conversions of AMP and BMI double bonds were quantified using the equations below:

$$Conv\ AMP = \frac{I_{790,printed\ or\ postcure}/I_{2850,printed\ or\ postcure}}{I_{790,resin}/I_{2850,resin}} \quad (2)$$

$$Conv\ BMI = \frac{I_{690,printed\ or\ postcure}/I_{2850,printed\ or\ postcure}}{I_{690,resin}/I_{2850,resin}} \quad (3)$$

The OCN (cyanate) group of the CE resin was characterized by a group of peaks at 2200-2300 cm^{-1}. The reaction of CE was confirmed by the disappearance of OCN group and presence of triazine ring represented by peaks 1360 cm^{-1} and 1558 cm^{-1}.

3. RESULTS

Poly(phenylmethane) dissolved well in AMP without recrystallizing after cooling to room temperature from 70°C. Although 50 wt% of this BMI can be dissolved in AMP, a mixture containing 30 % BMI in AMP was selected for the study as it possesses sufficiently low viscosity for printing. The selected cyanate ester also possesses low viscosity so that the IPN formulation could also be printed. This IPN formulation has the viscosity of 125 c.Ps, which is easy for DLP processing.

3.1 Resin characterization

Working curves were obtained in order to assess the depth of penetration (D_p), critical energy (E_c) for the systems investigated, and appropriate print times. Figure 2A shows cure depth vs energy on a semi-log plot for both resin systems investigated. The slope of the best-fit line to these data is D_p, and the intercept is the product of $-D_p*\ln(E_c)$ which allows for the determination of E_c. Values of D_p and E_c for the two systems are also shown in Figure 2A. The D_p of the IPN system is higher due to lower concentration of BMI, and a higher E_c is observed because of the dilution CE effect. The UV-VIS spectra of these two systems (Figure 2B) shows that BMI absorbs light at 405 nm, while AMP and n-CE do not. Therefore, BMI acts as a reactant as well as a light absorber. With a lower concentration of BMI, the IPN has higher D_p. The resins were printed using the same exposure time of 80 s and layer thickness of 100 microns. The same exposure time was used for the purpose of comparing conversion even though the BMI-AMP system could adequately be printed at lower exposure time.

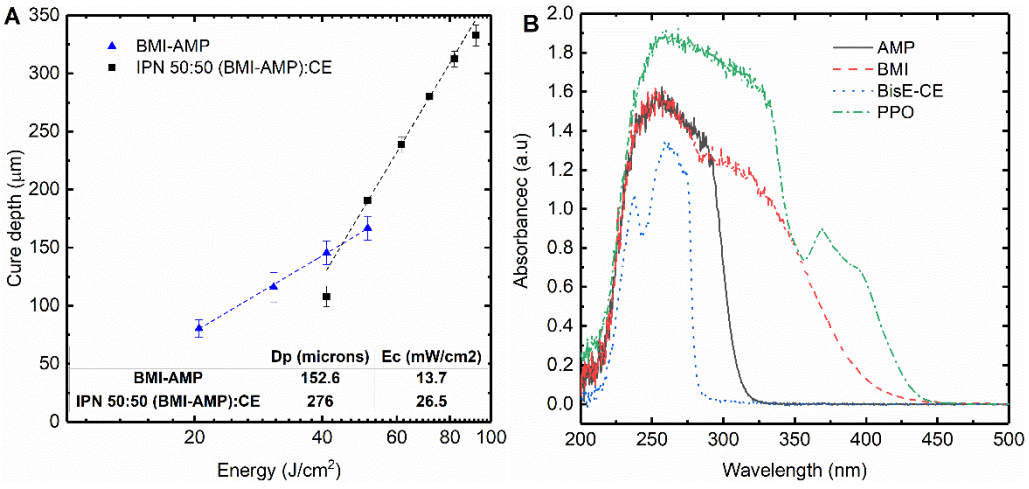


Figure 2: (A) Working curve of the resins, (B) UV-VIS spectra of individual components in the resins.

3.2 Dynamic mechanical analysis and volumetric shrinkage

Figure 3A and 3B show the storage modulus and loss modulus vs. temperature of the samples at different curing stages for the BMI-AMP and IPN systems, respectively. The corresponding conversions at various stages of cure are also given in these figures. The as-printed BMI-AMP system shows a T_g close to room temperature based on storage modulus. Therefore, this system reaches vitrification at room-temperature reaction conditions. The loss modulus curve shows a second peak at higher temperature which can be attributed to continued reaction during DMA testing. The as-printed IPN, on the other hand, has a T_g below 0 °C. This is due to the plasticizing effect of unreacted cyanate ester in the network. The conversion of BMI and AMP was calculated according to equation (2) and (3). It is observed that the conversion of BMI and AMP of the as printed IPN is significantly higher than that of the BMI-AMP system thus indicating vitrification is delayed for the IPN system, providing a less diffusion limited environment for the reaction between AMP and BMI to reach higher conversion. The T_g of the IPN system following the print stage is significantly lower than the cure temperature. This indicates that further reaction is possible if higher energy doses (exposure time) were applied. The UV-oven curing step for the IPN resulted in complete conversion of AMP and 52% conversion of BMI. Although curing was conducted at 75 °C, the T_g of the material remained below room temperature. For both systems, conversion and T_g increase significantly after thermal post-curing.

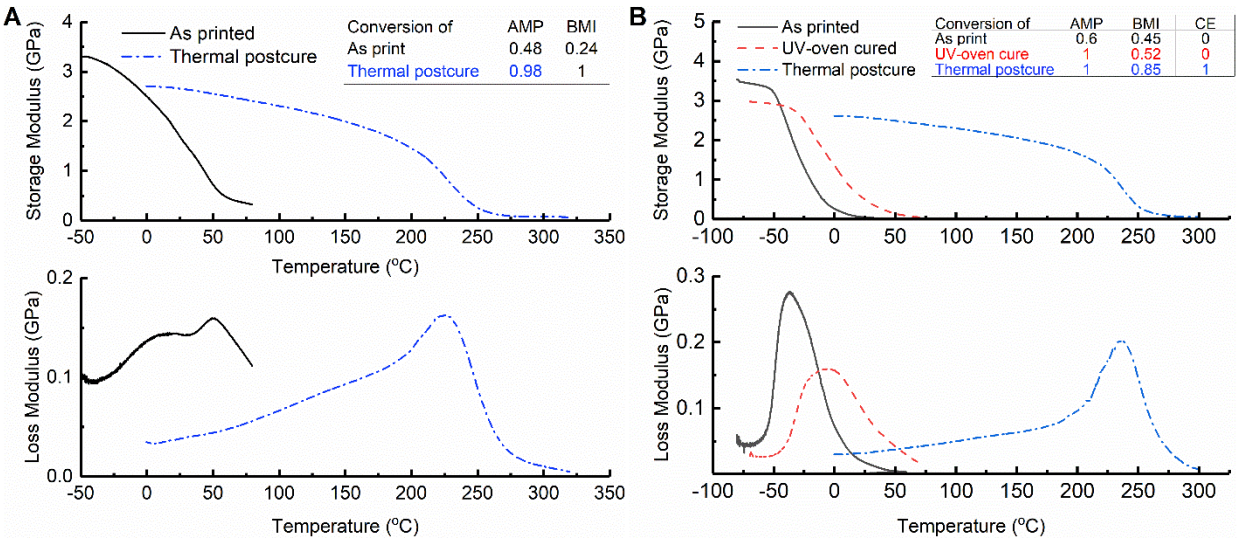


Figure 3: The storage and loss modulus vs. temperature at different stages of (A) BMI-AMP system, (B) IPN 50:50 (BMI-AMP):CE system

The final post-cure T_g of the IPN system is 236 °C, as defined by the peak position of the loss modulus curve. The T_g by tan delta is 260 °C, which is higher than current values reported in literatures.[5-6] The T_g by loss modulus for IPN system is compared with that estimated using the Fox equation:

$$\frac{1}{T_{g,f}} = \frac{w_1}{T_{g,1}} + \frac{w_2}{T_{g,2}} \quad (4)$$

Where $T_{g,f}$ is the final T_g of the IPN, $T_{g,1}$ is the T_g of BMI-AMP system, and $T_{g,2}$ is the T_g of pure CE system, w_1 is the weight fraction of BMI-AMP, and w_2 is weight fraction of CE. The T_g values defined above and the estimated T_g of the IPN are summarized in Table 1. The estimated T_g of the IPN is higher than the measured value by 15 °C. This could be due to a small amount of unreacted BMI in the system.

Table 1: The T_g of individual network and estimated T_g of IPN.

Material	T_g (°C)
BMI-AMP	225
IPN 50:50 (BMI-AMP):CE	236
Pure CE	280
Estimated T_g for IPN through Fox Equation	251

The volumetric shrinkage was calculated according to equation (1). Table 2 shows the density of materials at each stage and the accompanying volumetric shrinkage after post-cure relative to the unreacted resin. The volumetric shrinkage of the IPN after printing is roughly half that of the BMI-AMP system. The IPN also exhibits lower overall shrinkage after post-cure. Interestingly, the change in density between print and post-cure of the BMI-AMP sample is lower than the change in conversion would suggest. Why this is the case is an open question that merits further investigation. Possible reasons include mass loss during post-cure and physical constraints on shrinking imposed by vitrification at lower temperature. The observed lower shrinkage of the IPN as well as having a low modulus after printing could reduce residual stresses of the printed part.

Table 2: Density and % volumetric shrinkage of BMI-AMP and IPN system.

Density (g/cm^3)	BMI-AMP	IPN 50:50 (BMI-AMP):CE
Resin	1.1748	1.1780
As printed	1.2757	1.2340
Thermal post-cure	1.2817	1.2571
% Volumetric shrinkage as print vs. unreacted resin	8.58	4.58
% Volumetric shrinkage post-cure vs. unreacted resin	9.1	6.71

3.3 Mechanical properties

Compact tension and 3-point bending tests were carried out to examine fracture toughness and flexural properties, respectively. Figure 4A shows the critical strain energy release rate (G_{Ic}) and critical stress intensity factor (K_{Ic}) of the two systems. Bismaleimide is known to be brittle because of its high crosslinking density.[14] The low fracture toughness of BMI-AMP is expected. The IPN has significantly higher fracture toughness compared to the BMI-AMP system. This observation

is in agreement with reports in the literature that IPN network architectures result in toughened systems.[22-24] The reported G_{Ic} of pure bisphenol E cyanate ester is 190 J/m^2.[15] The IPN increases the toughness of BMI-AMP system but to a level lower than that of the pure cyanate ester system. Figure 4B shows the flexural strength and modulus of the BMI-AMP and IPN materials. Both systems possess good flexural properties. The flexural moduli are similar, but the IPN system has significantly higher flexural strength. The resulting IPN has good mechanical properties in addition to thermal properties.

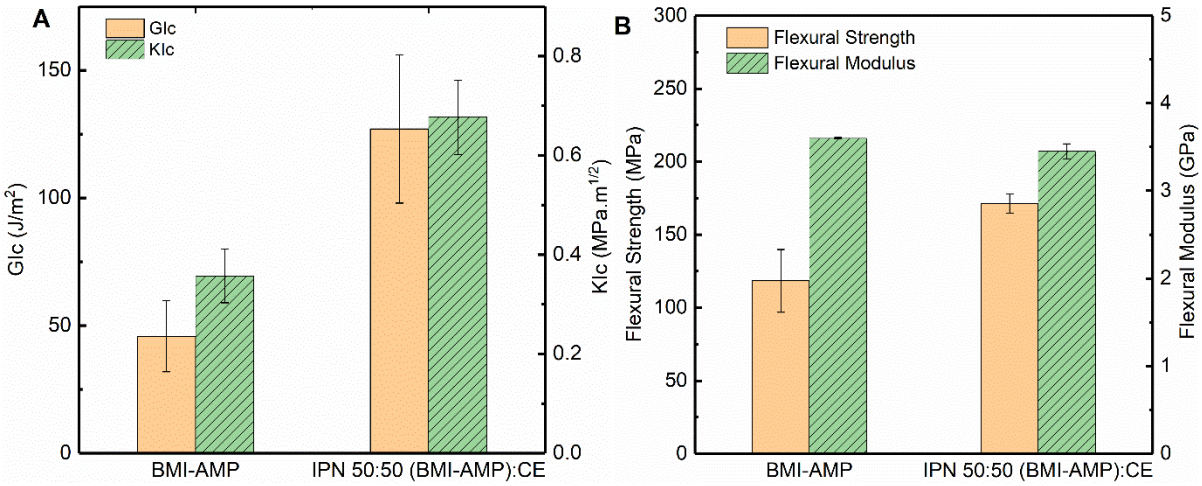


Figure 4: (A) Fracture toughness, (B) Flexural properties of BMI-AMP and IPN system.

4. CONCLUSIONS

This investigation demonstrated that high-performance thermosetting materials can be printed using stereolithography by formulating *in-situ* sequential IPN networks of BMI and CE. A copolymerization reaction between bismaleimide and a diluent occurs during printing, resulting in a cyanate ester swollen network with sub room temperature glass transition temperature (T_g). The polymerization of cyanate ester takes place during post processing. The resulting material possesses a T_g close to 240 ºC (loss modulus peak), significant decrease in cure shrinkage, high strength, and improved toughness.

5. ACKNOWLEDGEMENTS

Research was sponsored by the Army Research Laboratory and was accomplished under Cooperative Agreement Number W911NF-14-2-0227. The views and conclusions contained in this document are those of the authors and should not be interpreted as representing the official policies, either expressed or implied, of the Army Research Laboratory or the U.S. Government. The U.S. Government is authorized to reproduce and distribute reprints for Government purposes notwithstanding any copyright notation herein.

6. REFERENCES

[1] Guo N. and Leu M. C., "Additive manufacturing: technology, applications and research needs," *Frontiers of Mechanical Engineering,* vol. 8, no. 3, pp. 215-243, 2013. DOI: 10.1007/s11465-013-0248-8

[2] Ligon S. C., Liska R., Stampfl J., Gurr M., and Mülhaupt R., "Polymers for 3D printing and customized additive manufacturing," 2017. DOI: 10.1021/acs.chemrev.7b00074

[3] Chandrasekaran S., Duoss E. B., Worsley M. A., and Lewicki J. P., "3D printing of high performance cyanate ester thermoset polymers," *Journal of Materials Chemistry A,* vol. 6, no. 3, pp. 853-858, 2018. DOI: 10.1039/C7TA09466C

[4] Hegde M. *et al.*, "3D printing all-aromatic polyimides using mask-projection stereolithography: processing the nonprocessable," *Advanced Materials,* vol. 29, no. 31, p. 1701240, 2017. DOI: 10.1002/adma.201701240

[5] Zhang X., Xu Y., Li L., Yan B., Bao J., and A. Zhang, "Acrylate-based photosensitive resin for stereolithographic three-dimensional printing," *Journal of Applied Polymer Science,* vol. 136, no. 21, p. 47487, 2019. DOI: 10.1002/app.47487

[6] Kuang X., Zhao Z., Chen K., Fang D., Kang G., and Qi H. J., "High-Speed 3D Printing of High-Performance Thermosetting Polymers via Two-Stage Curing," *Macromolecular rapid communications,* vol. 39, no. 7, p. 1700809, 2018. DOI: 10.1002/marc.201700809

[7] Bychkov P., A. Chentsov, Kozintsev V., and Popov A., "Determination of residual stresses in objects at their additive manufacturing by layer-by-layer photopolymerization method," in *Journal of Physics: Conference Series*, 2018, vol. 991, no. 1, p. 012016: IOP Publishing.

[8] Karalekas D., Rapti D., Gdoutos E., and Aggelopoulos A., "Investigation of shrinkage-induced stresses in stereolithography photo-curable resins," *Experimental mechanics,* vol. 42, no. 4, pp. 439-444, 2002. DOI: 10.1007/BF02412150

[9] Shah D. U. and Schubel P. J., "Evaluation of cure shrinkage measurement techniques for thermosetting resins," *Polymer Testing,* vol. 29, no. 6, pp. 629-639, 2010. DOI: 10.1016/j.polymertesting.2010.05.001

[10] Palmese G. and Gillham J., "Time–temperature–transformation (TTT) cure diagrams: Relationship between Tg and the temperature and time of cure for a polyamic acid/polyimide system," *Journal of applied polymer science,* vol. 34, no. 5, pp. 1925-1939, 1987. DOI: 10.1002/app.1987.070340511

[11] Lange J., Toll S., Månson J.-A. E., and Hult A., "Residual stress build-up in thermoset films cured above their ultimate glass transition temperature," *Polymer,* vol. 36, no. 16, pp. 3135-3141, 1995. DOI: 10.1016/0032-3861(95)97876-H

[12] Li W., Noodeh M. B., Delpouve N., Saiter J.-M., Tan L., and Negahban M., "Printing continuously graded interpenetrating polymer networks of acrylate/epoxy by manipulating cationic network formation during stereolithography," *Express Polymer Letters,* vol. 10, no. 12, 2016.

[13] Sitzmann E. V., Anderson R. F., Koljack M. P., Cruz J. G., and Srivastava C. M., "High temperature performance polymers for stereolithography," ed: Google Patents, 2000.

[14] Iredale R. J., Ward C., and Hamerton I., "Modern advances in bismaleimide resin technology: A 21st century perspective on the chemistry of addition polyimides," *Progress in Polymer Science,* vol. 69, pp. 1-21, 2017. DOI: 10.1016/j.progpolymsci.2016.12.002

[15] Hamerton I. and Hay J. N., "Recent developments in the chemistry of cyanate esters," *Polymer international,* vol. 47, no. 4, pp. 465-473, 1998. DOI: 10.1002/(SICI)1097-0126(199812)47:4<465::AID-PI88>3.0.CO;2-S

[16] Nair C. R., Mathew D., and Ninan K., "Cyanate ester resins, recent developments," in *New Polymerization Techniques and Synthetic Methodologies*: Springer, 2001, pp. 1-99.

[17] Gu A., "High performance bismaleimide/cyanate ester hybrid polymer networks with excellent dielectric properties," *Composites Science and Technology,* vol. 66, no. 11-12, pp. 1749-1755, 2006. DOI: 10.1016/j.compscitech.2005.11.001

[18] Geng X., "Bismaleimide and cyanate ester based sequential interpenetrating polymer networks for high temperature application," 2005.

[19] Hamerton I., "High-performance thermoset-thermoset polymer blends: A review of the chemistry of cyanate ester-bismaleimide blends," *High performance polymers,* vol. 8, no. 1, pp. 83-95, 1996. DOI: 10.1088/0954-0083/8/1/006

[20] Fan S., Boey F., and Abadie M., "UV curing of a liquid based bismaleimide-containing polymer system," *Exp Polym Lett,* vol. 1, pp. 397-405, 2007. DOI: 10.3144/expresspolymlett.2007.56

[21] Francis L., McCormick A., Vaessen D., and Payne J., "Development and measurement of stress in polymer coatings," *Journal of Materials Science,* vol. 37, no. 22, pp. 4717-4731, 2002. DOI: 10.1023/A:1020886802632

[22] Ligon-Auer S. C., Schwentenwein M., Gorsche C., Stampfl J., and Liska R., "Toughening of photo-curable polymer networks: a review," *Polymer Chemistry,* vol. 7, no. 2, pp. 257-286, 2016. DOI: 10.1039/C5PY01631B

[23] Sperling L. H., "Interpenetrating polymer networks: an overview," ACS Publications, 1994. DOI: 10.1021/ba-1994-0239.ch001

[24] Lin M. S., Liu C. C., and Lee C. T., "Toughened interpenetrating polymer network materials based on unsaturated polyester and epoxy," *Journal of Applied Polymer Science,* vol. 72, no. 4, pp. 585-592, 1999. DOI: 10.1002/(SICI)1097-4628(19990425)72:4<585::AID-APP15>3.0.CO;2-M